# Small Nuclear Reactors in Microgrids: Modeling and Flexibility Provision

Yemi Ojo, Bikash Poudel, Timothy R. McJunkin, and Ning Kang
*Power and Energy Systems Department*
*Idaho National Laboratory*
Idaho Falls, United States
yemi.ojo@inl.gov, bikash.poudel@inl.gov, timothy.mcjunkin@inl.gov, ning.kang@inl.gov

***Abstract*—Recent advances in technology with compact design, modularity, and enhanced safety features make small nuclear reactors well-suited for microgrid applications. To support their safe deployment in microgrids, this paper presents a modeling framework that can be used to investigate the behavior of small nuclear reactors in microgrids and test controls designed to provide flexibility. Under the framework, a small reactor model is developed that enables testing with high-fidelity representation of the system components without putting one-of-a-kind equipment at risk. To enhance flexibility, a grid-forming battery is modeled to support small nuclear reactors with load-following capabilities. The models are built in a Real Time Digital Simulator, allowing real-time validations and supporting transitioning from simulation to hardware testing. Real-time simulations show that the grid-forming battery supports the small nuclear reactor with load-following capabilities.**

***Index Terms*—Microgrids, small nuclear reactor, grid-forming battery storage, load-following**

## I. Introduction

Grid resilience is a global concern, prompting efforts to decentralize power grids. Deploying microgrids which can operate off the main grid support this goal by integrating distributed energy sources to meet local load needs and enabling the reconfiguration of large networks into manageable sections. However, these energy sources are often variable, causing intermittencies that require microgrids operators to balance mismatches for grid stability.

Small nuclear reactors[1] address these challenges with benefits like dispatchability (as compared to variable energy resources), compact size, high reliability, and long fueling cycles, allowing multiple years of operation before refueling [1], [2]. While smaller-capacity reactors were historically used in naval propulsion and research, recent advances in modularity and safety features now make them viable for microgrids [3], [4]. Small nuclear reactors offer features that support microgrids applications, such as flexibility through modular design (can operate with some modules turned on/off) and ability to change their power output. Notable microgrid compatible technologies under development include the eVinci™ SMR (5 MWe)[2] that features an autonomous design that can provide load-following, grid frequency control, and black start capability using both control drums and rods [3]. The GE-Hitachi BWRX-300 reactor uses advanced techniques for precise control during normal operation and rapid hydraulic insertion of control rods during emergencies [5]. The NuScale SMR can load-follow by using NuFollow™ and multi-module design that allow flexible power output [6], [7].

However, two issues arise with using small nuclear reactors in microgrids. First, although newer designs promise load-following flexibilities, frequent power adjustments for all grid scenarios can be costly and thermally stressful for the system. While studies pairing small nuclear reactors with batteries exist [8], integration with grid-forming batteries is under reported. Second, there is limited experience with using small nuclear reactors in microgrids, and experimenting with this one-of-a-kind equipment can be risky and costly.

To address the first problem, we propose that grid-forming batteries are used to support the reactors with load-following capabilities. These battery systems use inverters with grid-forming control that can set and maintain frequency and voltage (mimicking traditional generators), establish standalone grids, and improve stability. Grid-forming strategies include droop control, matching control, and virtual synchronous generators [9]. To address the second issue, we propose a modeling framework that researchers can use to evaluate the performance of small nuclear reactors in microgrids and test control strategies aimed to provide flexibility. This enables real-time simulations that can identify integration challenges well before a physical reactor is built and tested, supports a gradual transition from simulation to hardware testing, and allows researchers to assess whether the system architecture, asset mix, and control are appropriately configured for first-of-a-kind deployment. The modeling framework can be adapted for modeling a wide range of nuclear technologies and microgrids topologies. Because all parts of the system can be simulated in real-time, it can easily be reconfigured to incorporate both simulated and physical distributed energy assets. To summarize the contributions, this paper:

1) Develops a small reactor model described by neutronics, gas-Brayton heat transfer mechanism, and power conversion systems. This allows testing in microgrids with high-fidelity representation of the reactor components without putting one-of-a-kind equipment at risk.
2) Models a grid-forming battery supporting small nuclear reactors by setting and maintaining grid frequency and

This work is authored by Battelle Energy Alliance, LLC under Contract No. DE-AC07-05ID14517 with the U.S. Department of Energy (DOE). This work is supported through the DOE Office of Electricity Microgrid Program.

[1]Small nuclear reactors include Small Modular Reactors (SMRs) and microreactors

[2]MWe means MW electrical

979-8-3315-8138-1

voltage and providing load-following by absorbing excess power or supplying energy during shortages.

3) Builds the models in a Real Time Digital Simulator (RTDS) to facilitate real-time simulations and assist in transitioning from simulation to hardware testing.

The real-time simulations performed in RTDS shows that grid-forming batteries can support the reactor with load-following capabilities.

The remainder of the paper is organized as follows. Section II presents the modeling framework. Sections III and IV describe the small reactor and grid-forming battery models. Section V presents discussions and real-time results, followed by conclusion and future work in section VI.

## II. Modeling Framework

This section presents the nuclear microgrid modeling framework (Fig. 1). The nuclear microgrid is composed of the small reactor model, grid-forming battery model, and the microgrid network. Let $x_{\text{sr}}(t) \in \mathbb{R}^{x_s}, u_{\text{sr}} \in \mathbb{R}^{u_s}$ denote the state and input signals of the reactor model, $y_{\text{bs}}(t) \in \mathbb{R}^{y_b}, u_{\text{bs}}(t) \in \mathbb{R}^{u_s}$ the state and input signals of the grid-forming battery model, and $u_{\text{mg}}(t) \in \mathbb{R}^{u_m}, y_{\text{mg}} \in \mathbb{R}^{y_m}$ the state and input signals of the microgrid. These nuclear microgrid components interact through the exchange of signals, $y_{\text{sr}}(t) \in \mathbb{R}^{y_s}, y_{\text{bs}}(t) \in \mathbb{R}^{y_b}, y_{\text{mg}}(t) \in \mathbb{R}^{y_m}$, respectively. Each system is assumed to be nonlinear and can generally be described using ordinary differential equations. The state-space model can be described as

$$\begin{aligned} \dot{x}_{\text{sr}} &= f_{\text{sr}}(x_{\text{sr}}, u_{\text{sr}}) \\ y_{\text{sr}} &= h_{\text{sr}}(x_{\text{sr}}), \quad u_{\text{sr}} = h_{\text{sr}}(y_{\text{mg}}) \end{aligned} \tag{1}$$

$$\begin{aligned} \dot{x}_{\text{bs}} &= f_{\text{bs}}(x_{\text{bs}}, u_{\text{bs}}) \\ y_{\text{bs}} &= h_{\text{bs}}(x_{\text{bs}}), \quad u_{\text{bs}} = h_{\text{bs}}(y_{\text{mg}}) \end{aligned} \tag{2}$$

$$\begin{aligned} \dot{x}_{\text{mg}} &= f_{\text{bs}}(x_{\text{mg}}, u_{\text{mg}}) \\ (y_{\text{mg}}, \hat{y}_{\text{mg}}) &= h_{\text{bs}}(x_{\text{mg}}), \quad u_{\text{mg}} = g_{\text{sr}}(y_{\text{sr}}, y_{\text{bs}}). \end{aligned} \tag{3}$$

Equations (1), (2), (3) represent the small reactor, grid-forming battery, and microgrid systems, respectively. The functions, $f_{\text{sr}}, h_{\text{sr}}, f_{\text{sr}}, f_{\text{bs}}, h_{\text{bs}}, f_{\text{bs}}, f_{\text{mg}}, h_{\text{mg}}, f_{\text{mg}}$, are continuous and are time invariant. These models are developed in RTDS for real-time simulations, allowing to transition to hardware testing by substituting models with physical assets. The benefit of the modeling framework is that it is adaptable for modeling various nuclear microgrids, with RTDS simulations offering valuable insights and flexible system integrations.

We present below particular models describing the small nuclear reactor and grid-forming battery. Afterwards, the states, inputs, and outputs corresponding to those in (1), (2), (3) are identified (Section V-A).

## III. Small Reactor Model

The small reactor features a gas-cooled, single-loop design combining neutronics, a gas-Brayton heat transfer mechanism, and a power conversion system (Fig. 2) [10]. The heat exchanger represents the reactor core; the gas-Brayton cycle consists of a compressor, turbine, recuperator, and radiator; and the power conversion includes the generator. Gas is preheated in the recuperator, compressed, heated by the core

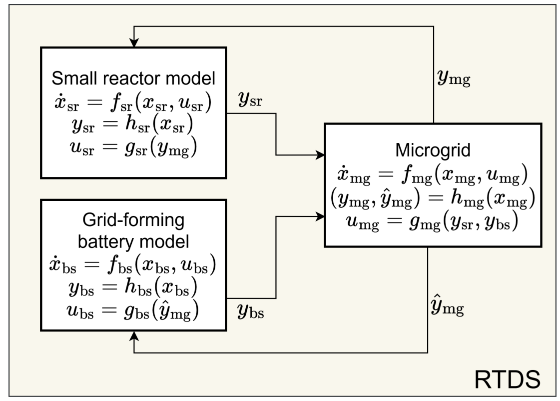


Fig. 1. Nuclear microgrid modeling framework

(heat exchanger), expanded in the turbine, passed back through the recuperator, and finally cooled in the radiator. $T_{o1}$ is the compressor inlet/radiator outlet; $T_{o2}$ is the recuperator inlet/compressor outlet; $T_{o3}$ is the reactor inlet/recuperator outlet; $T_{o4}$ is the turbine inlet/reactor outlet; $T_{o5}$ is the recuperator high-temperature inlet/turbine outlet; and $T_{o6}$ is the waste heat rejection inlet/recuperator high-temperature outlet.

The systems for the small reactor–neutronics, gas-Brayton, and power conversion– are described below. The model is easily adaptable for a wide range of nuclear technologies. With minimal parametric changes, the RTDS-based model can simulate various small nuclear reactor designs, heat transfer systems, and power conversion units. For example, point kinetics equations are used to model reactor dynamics, allowing quick adaptation to different core behaviors. Likewise, the gas-Brayton thermal system can be tuned or swapped to reflect alternatives such as Rankine or Stirling cycles.

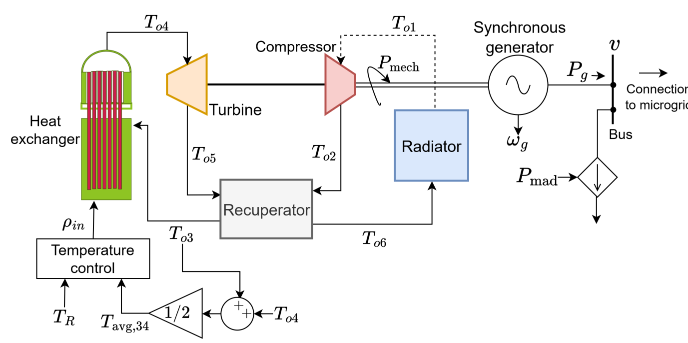


Fig. 2. Small nuclear reactor system

### A. Neutronics

The reactor's neutronics are described by the point kinetic equations, assuming stable power distribution and neutron flux that are proportional to the heat produced, $P_{rx}$. The model includes a negative feedback term, $\alpha$, which accounts for fuel temperature-related reactivity changes. Reactor power increases with positive reactivity ($\rho$) and decrease with negative reactivity. The lumped point kinetics model is as follows:

$$\dot{P}_{rx} = \left(\frac{\rho - \beta}{\Lambda}\right) P_{rx} + \lambda C \tag{4a}$$

$$\dot{C} = \frac{\beta}{\Lambda} P_{rx} - \lambda C \tag{4b}$$

$$m_r c_p \dot{T}_{o4} = -P_{rx} - P_{th} \tag{4c}$$

979-8-3315-8138-1

$$\dot{T}_f = k_f P_{rx} - \gamma_f (T_f - T_{\text{avg},34}) \quad (4d)$$
$$\rho = \rho_{in} - \alpha T_f \quad (4e)$$
$$P_{th} = \dot{m}_r (T_{o4} - T_{o3}) \quad (4f)$$
$$T_{\text{avg},34} = \frac{T_{o4} - T_{o3}}{2} \quad (4g)$$
$$\dot{\psi} = T_{\text{avg},34} - T_R \quad (4h)$$
$$\rho_{in} = -K_P (T_{\text{avg},34} - T_R) - K_I \psi. \quad (4i)$$

$\beta$ is the total delayed neutron fraction, $\Lambda$ is the prompt neutron generation time, $C$ is the concentration of delayed neutrons group, and $\rho_{in}$ is the reactivity inserted. $K_P, K_I$ are the proportional and integral gains and $T_R, T_f$ are the reactor fuel desired reference and average temperatures. $K_f$ is the fuel inverse thermal capacitance, $\gamma_f$ is the heat transfer inverse time constant from fuel to coolant, $T_{\text{avg},34}$ is the reactor average inlet and outlet temperatures, and $c_p$ is the coolant heat capacity. $m_r, \dot{m}_r$ refer to the core mass and mass flow rate. The reactor becomes critical when $\rho = 0$, meaning that inserted reactivity in (4e) sets the fuel temperature (i.e., $\rho_{in} = \alpha_f T_f$).

Furthermore, a temperature control (4h)-(4i) is incorporated which ensures that the core average temperature, $T_{\text{avg},34}$, is maintained at a setpoint, $T_R$. Reactivity affects power by adjusting the fuel average temperature $T_f$, to maintain $T_{\text{avg},34} - T_R = 0$.

### B. Gas-Brayton System

The gas-Brayton system includes a compressor, turbine, recuperator, and radiator. The compressor raises the gas pressure by $r_{pc}$, causing temperature to increase (5a) and work, $\dot{W}_c$, as in (5b).

$$T_{o2} = T_{o1} + \frac{T_{o1}}{\eta_c}\left(r_{pc}^{\frac{\gamma-1}{\gamma}} - 1\right) \quad (5a)$$
$$\dot{W}_c = \dot{m}_r c_p (T_{o1} - T_{o2}) \quad (5b)$$

$\gamma$ is the heat capacities ratio at constant pressure and volume and $\eta_c$ is the compression isentropic efficiency. The recuperator preheats the gas exiting the compressor by

$$T_{o3} = \xi_x (T_{o5} - T_{o2}) + T_{o2} \quad (6)$$

where $\xi_x$ is the effectiveness of the recuperator. Furthermore, the turbine lowers the gas pressure by $r_{pc}$, causing temperature to fall (7a) and work, $\dot{W}_t$, as in (7b).

$$T_{o5} = T_{o4} + \eta_c T_{o4}\left(1 - r_{pt}^{\frac{\gamma-1}{\gamma}}\right) \quad (7a)$$
$$\dot{W}_t = \dot{m}_r c_p (T_{o1} - T_{o2}) \quad (7b)$$

$\eta_c$ is the compression isentropic efficiency.

### C. Power Conversion System

Mechanical power, $P_m$, is generated through the work done by the compressor and turbine as epressed in

$$P_m = \dot{W}_c + \dot{W}_t. \quad (8)$$

Suppose the reactor includes an auxiliary power management system, it can be represented by

$$P_{\text{mad}} = -\hat{K}_P (\omega_g - \omega_n), \quad (9)$$

Thus, the generator swing equation can be described as

$$M\dot{\omega}_g = -D\omega_g + P_m + P_{\text{mad}} - P_g \quad (10)$$

where $P_g$ denotes the power delivered to the grid. For completeness, the power conversion system typically include the electrical dynamics of the synchronous generator, which is omitted here due to page constraints. Nonetheless, with its excitation system included, the generator model can be represented as

$$\dot{x}_{\text{sg}} = f_{\text{sg}}(x_{\text{sg}}, u_{\text{sg}}), \quad u_{\text{sg}} = h_{\text{sg}}(y_{\text{mg}}) \quad (11)$$

where $x_{\text{sg}}, u_{\text{sg}}$ are the state and input signals, respectively. $P_g = u_{\text{sg}}^\top x_{\text{sg}}^{(v)}$, where $x_{\text{sg}}^{(v)} \in x_{\text{sg}}$ corresponds to the generator terminal (bus) voltage. Hence, (4)-(11) gives the small reactor model.

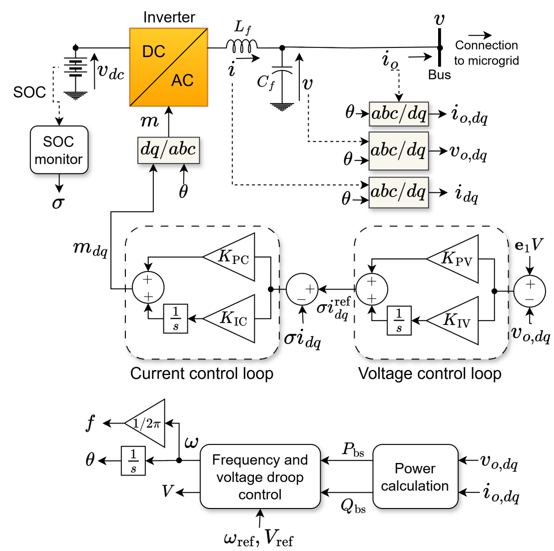


Fig. 3. Grid-forming battery storage system.

## IV. Grid-Forming Battery Model

This section describes the grid-forming battery system (Fig. 3) comprising a DC-side battery, three-phase inverter, current and voltage control loops, state of charge (SOC) monitor, and an AC-side that has an $LC$ filter with inductance, $L_f$, and a shunt capacitance and conductance, $C_f$. The input current, $i$, output voltage, $v_o$, and modulating signal, $m$, are balanced three-phase sinusoids. Applying the Park ($dq/abc$) transform (see e.g., [11]) to the inverter three-phase ($abc$) average model, the direct-quadrature ($dq$) representation is given by

$$\begin{aligned} L_f \dot{i}_{dq} &= (-R_f \mathbf{I}_2 + \omega_{bs} L_f J) i_{dq} + \frac{1}{2} m_{dq} v_{dc} - v_{o,dq} \\ C_f \dot{v}_{o,dq} &= (-G_f \mathbf{I}_2 + \omega_{bs} C_f J) v_{o,dq} + i_{dq} - i_{o,dq} \end{aligned} \quad (12)$$

where $\mathbf{I}_2$ is an identity matrix of size 2, and $J = \begin{bmatrix} 0 & 1 \\ -1 & 0 \end{bmatrix}$. $R_f$, $G_f$ are the resistance and conductance of the inductor, $L_f$, and capacitor, $C_f$. $i_{dq}, v_{o,dq}, m_{dq}$ are, respectively, 2-dimensional inverter current, $i$, voltage, $v_o$, and modulating signal, $m$. $\omega_{bs}$ denotes the frequency. A grid-forming strategy is used to compute $\omega_{bs}$ and $m_{dq}$ as described below.

The frequency, $\omega_{bs}$, is controlled through the conventional droop control [9], which by using the inverter active power output, $P_{bs}$, adjusts the frequency setpoint, $\omega_n$, as in (13b).

Similarly, voltage droop is implemented by adjusting the voltage setpoint, $V_n$, using the inverter reactive power output, $Q_{bs}$, as in (13b).

$$\tau\dot{\omega}_{bs} = -\omega_{bs} + \omega_n - \bar{k}_p P_{bs} \quad (13a)$$
$$\tau\dot{V}_{bs} = -V_{bs} + V_n - \bar{k}_p Q_{bs} \quad (13b)$$

$\tau$ is the low pass filters time constant and $\bar{k}_p, \bar{k}_q$ are the droop gains, $P_{bs} = v_{o,dq}^\top i_{o,dq}$ and $Q_{bs} = v_{o,dq}^\top J^\top i_{o,dq}$.

The modulating signal, $m_{dq}$, is computed through the nested current (14c)-(14d) and voltage control (14a)-(14b) loops, as follows

$$\dot{\chi}_{dq} = v_{o,dq} - \mathbf{e}_1 V_{bs} \quad (14a)$$
$$i_{dq}^{\text{ref}+-} = -K_{\text{PV}}(v_{o,dq} - \mathbf{e}_1 V_{bs}) - K_{\text{IV}}\chi_{dq} \quad (14b)$$
$$\dot{\zeta}_{dq} = \sigma(i_{dq} - i_{dq}^{\text{ref}+-}) \quad (14c)$$
$$m_{dq} = -\sigma K_{\text{PC}}(i_{dq} - i_{dq}^{\text{ref}+-}) - K_{\text{IC}}\,\zeta_{dq}, \quad (14d)$$

with integrator states, $\chi_{dq}, \zeta_{dq}$, proportional gains, $K_{\text{PV}}, K_{\text{PC}}$, integral gains, $K_{\text{IV}}, K_{\text{IC}}$, $\mathbf{e}_1 = [1 \ \ 0]^\top$, and SOC sensing function, $\sigma$. Regulating the deviation, $v_{o,dq} - \mathbf{e}_1 V$, to zero in (14a)-(14b) causes the inverter output voltage to track the reference. Consequently, the reference current, $i_{dq}^{\text{ref}}$, is produced which tracked by $i_{dq}$ in (14c)-(14d) generates $m_{dq}$. The $abc$ form of $m$ is obtained by performing the inverse Park transform $(dq/abc)$ of $m_{dq}$. The battery system may incorporate an SOC monitor with the sensing function, $\sigma$, defined by

$$\sigma = \begin{cases} 1 & \text{if } \underline{\text{SOC}} \le \text{SOC} \le \overline{\text{SOC}} \\ 0 & \text{otherwise.} \end{cases} \quad (15)$$

Including $\sigma$ in (14c)-(14d) ensures that the grid-forming battery injects or absorb power when the SOC lower and upper limits, $\underline{\text{SOC}}, \overline{\text{SOC}}$, are not violated.

Therefore, (12)-(15) describes the grid-forming battery. The grid-forming battery supports the small reactor with load-following, as demonstrated in the next section (Section V-C).

## V. Discussions and Real-Time Results

### A. Discussion on Modeling Framework

This section outlines the states, input, and outputs in the modeling framework (1), (2), (3). Clarifying which signals are exchanged helps streamline adaptation and simulation across various nuclear microgrid configuration.

To this end, the microgrid interconnects power lines and loads. As detailed in sources like [11], the microgrid output signals, $(y_{\text{mg}}, \hat{y}_{\text{mg}})$, represent the network current. According to these references, converting the network current to values at the buses requires premultiplying $(y_{\text{mg}}, \hat{y}_{\text{mg}})$ by $\mathcal{T}^{-1}(\delta)$ (where $\mathcal{T}(\delta) = [\cos\delta \ \ -\sin\delta; \ \ \sin\delta \ \ \cos\delta] \in \mathbb{R}^{2\times 2}$; $\mathcal{T}^{-1}(\delta) = \mathcal{T}^\top(\delta)$), with reverse transformation applied for the reverse operation. The bus angle, $\delta$, is determined by $\dot{\delta} = \omega_a - \omega_s$, where $\omega_a \in \{\omega_{bs}, \omega_g\}$ and $\omega_s$ serves as the reference frequency.

Therefore, for the small nuclear reactor (4)-(11), the state, input, and output vectors are defined as $x_{\text{sr}} = (P_{rx}, C, T_{o4}, T_f, \psi, \omega_g, x_{sg})$, $u_{\text{sr}} = \mathcal{T}^{-1}(\delta)y_{\text{mg}}$, and $y_{\text{sr}} = (x_{\text{sg}}^{(v)}, \omega_g)$. $x_{\text{sg}}^{(v)}$ refers to a state in $x_{\text{sg}}$ corresponding to the generator terminal (bus) voltage. $x_{\text{sg}}^{(v)} = v_{odq}$ if the reactor and battery connect to the same bus. For the grid-forming battery system, the state, input, and output are defined as $x_{\text{bs}} = (i_{dq}, v_{o,dq}, \omega_{bs}, V, \chi_{dq}, \zeta_{dq})$, $u_{\text{bs}} = \mathcal{T}^{-1}(\delta)\hat{y}_{\text{mg}} = i_{o,dq}$, and $y_{\text{bs}} = (v_{o,dq}, \omega_{bs})$.

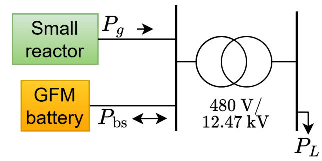


Fig. 4. A test system for small nuclear microgrid, with GFM denoting grid-forming battery.

### B. Discussion on RTDS Modeling

The RTDS model is built using the Power System and Controls libraries in RSCAD FX 2.6 (Real-Time Simulation Software Package). The neutronics and gas-Brayton system (4)-(8) in the small nuclear reactor model (4)-(11) are built using the integrator, constant, summer, and power blocks in the Controls library; and the synchronous generator with excitation (10)-(11) is modeled using the Power System library blocks If_rtds_sharc_sld_MACV31 (generator) and _rtds_EXST1A.def (IEEET1). The grid-forming battery (12)-(15) is modeled using battery_rtds_libat.def (battery) and If_rtds_sharc_sld_TRF3P2W (inverter), and the grid-forming control is implemented using the integrator, constant, and summer blocks in the Controls library. The microgrid network (transformer and load) is modeled using _rtds_3phAVMv1.def and dynamic load block rtds_udc_DYLOAD. Note that the network can also be modeled per case or using the IEEE benchmark examples. The simulation real-time step is $50\,\mu$s.

### C. Real-Time Simulation Results

This section tests whether the grid-forming battery supports the small reactor with load-following. The RTDS system is setup as above (Fig. 4), lumping the microgrid loads as $P_L + jQ_L$ and using the parameters in [10], [11], $T_{o1}$=395, $T_R$=947.5, $K_P$=100, and $K_I$=1. To test the grid-forming battery load-following ability, the small reactor is operated at a fixed power output, $P_g = 2$ MW (with $\hat{K}_P$=0). In Fig. 5, a load ($P_L$) step-down at $t = 6$ s from 2.5 MW to 1.5 MW shows the grid-forming battery absorbing the excess power, as indicated by $P_{bs}$=$-0.5$ MW and increasing SOC for $t > 6$ s. Conversely, in Fig. 6, a load ($P_L$) step-up at $t = 6$ s from 1.5 MW to 2.5 MW shows the grid-forming battery injecting additional power to balance the demand, as verified by $P_{bs}$=0.5 MW and decreasing SOC for time, $t > 6$ s. The frequencies ($f_g = \omega_g/2\pi$, $f_{bs} = \omega_{bs}/2\pi$) converge to the same value at steady state despite the load disturbance. Reactivity at $\rho = 0$ verifies that the reactor is critical and temperatures regulated with $T_{\text{avg},34}$ maintained reference, $T_R = 947.5$ (Fig. 7). These remain unchanged since the reactor is operated at a fixed power output.

## VI. Conclusion and Future Work

### A. Conclusion

Small nuclear reactors are becoming attractive for microgrids due to dispatchability/flexibility, reliability, compact size, and advanced safety features. To support their safe deployment

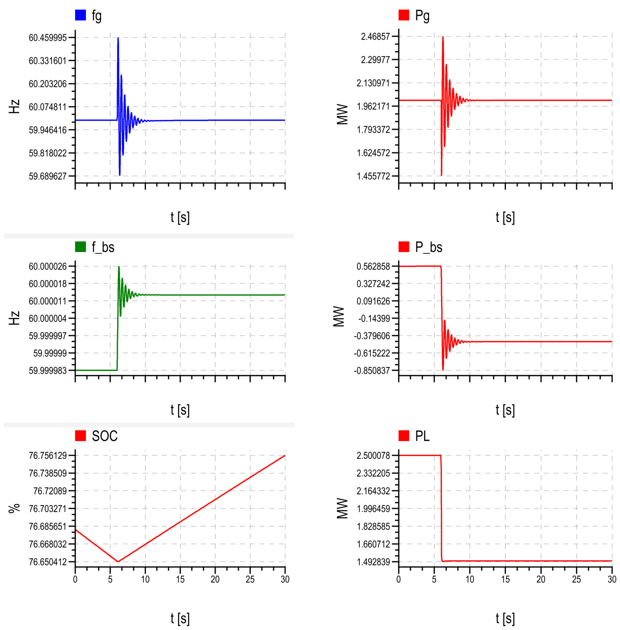


Fig. 5. Test 1: The load, $P_L$, steps down from 2.5 MW to 1.5 MW

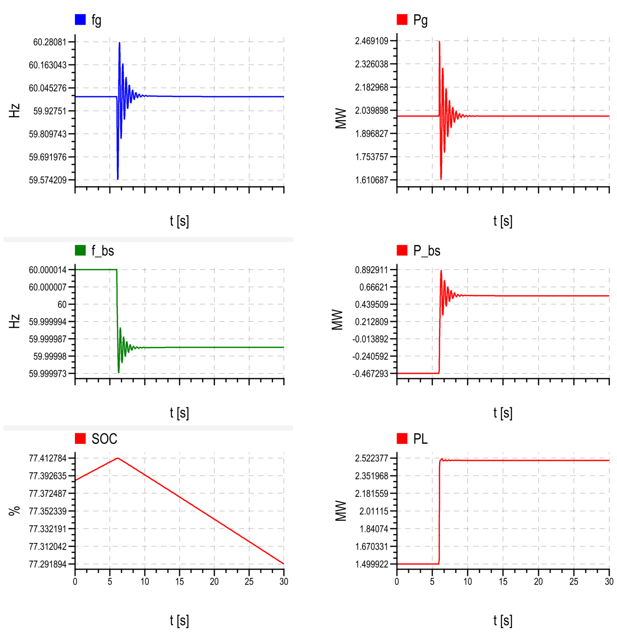


Fig. 6. Test 2: Load, $P_L$, steps up from 1.5 MW to 2.5 MW

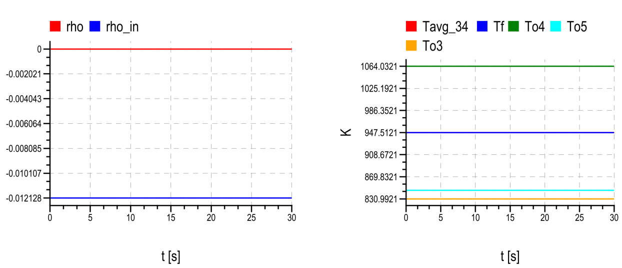


Fig. 7. Small reactor's reactivity and temperatures

in microgrids, this paper develops a modeling framework that can be used to investigate the behavior of small nuclear reactors in microgrids and validate controls meant to provide flexibility. Thus, a small reactor model has been presented that allows testing with high-fidelity representation of the system components without damaging a one-of-a-kind equipment. Flexibility is enhanced through a grid-forming battery modeled to support small nuclear reactors with load-following capabilities. The models are built in a RTDS to enable real-time testing and ease the transition from simulation to hardware testing. The real-time simulations show that the grid-forming battery supports the small reactor with load-following capabilities.

### B. *Future Work*

The proposed modeling framework implemented on the Idaho National Laboratory (INL)'s real-time simulation platform hosting RTDS will continue to evolve for validating nuclear microgrids. Future effort includes a gradual substitution of the small reactor model with assets like MAGNET and MARVEL (MAGNET: is an electrically heated thermal Microreactor Agile Non-nuclear Experimental Testbed; MARVEL: is a sodium-potassium-cooled microreactor expected to be operational at INL's Transient Reactor Test Facility in 2028), and the grid-forming battery model replaced by INL's Microgrid-in-a-Box. MACS (Microreactor Automatic Control System) will also be integrated to control MAGNET and MAVEL. This will support the safe, efficient and scalable deployment of small reactor energy systems under realistic grid conditions.

## References


[1] M. Nichol and H. Desai, "Cost competitiveness of micro-reactors for remote markets," *Nuclear Energy Institute (NEI): Washington, DC, USA*, 2019.

[2] A. Abou-Jaoude, Y. Arafat, A. W. Foss, and B. W. Dixon, "An economics-by-design approach applied to a heat pipe microreactor concept," Idaho National Lab.(INL), Idaho Falls, ID (United States), Tech. Rep., 2021.

[3] IAEA, "Advances in Small Modular Reactor Technology Developments. A Supplement to: IAEA Advanced Reactors Information System (ARIS): : Vienna, Austria," https://aris.iaea.org/Publications/, [Accessed November 10, 2025].

[4] C. Forsberg, A. Foss, and A. Abou-Jaoude, "Fission battery economics-by-design," *Progress in Nuclear Energy*, vol. 152, p. 104366, 2022.

[5] GE Vernova Hitachi, "BWRX-300 SMR," ww.gevernova.com/content/dam/gepower-new/global/en_US/images/gas-new-site/en/bwrx-300/fact-sheets/GEA34989B-BWRX-300-Fuel-Info-VernovaHitachi-Letter.pdf, [Accessed November 10, 2025].

[6] NuScale, "NuScale Power Module," https://www.nuscalepower.com/products/nuscale-power-module, [Accessed November 10, 2025].

[7] K. Park, T. Park, S. K. Zee, and B. S. Koo, "Control rod driven long-term load-follow operation in small modular reactor," *Annals of Nuclear Energy*, vol. 182, p. 109620, 2023.

[8] B. Poudel and R. Gokaraju, "Optimal operation of SMR-RES hybrid energy system for electricity & district heating," *IEEE Transactions on Energy Conversion*, vol. 36, no. 4, pp. 3146–3155, 2021.

[9] D. B. Rathnayake, M. Akrami, C. Phurailatpam, S. P. Me, S. Hadavi, G. Jayasinghe, S. Zabihi, and B. Bahrani, "Grid forming inverter modeling, control, and applications," *IEEE Access*, vol. 9, pp. 114 781–114 807, 2021.

[10] S. A. Wright, R. J. Lipinski, M. E. Vernon, and T. Sanchez, "Closed brayton cycle power conversion systems for nuclear reactors," Sandia National Lab.(SNL-NM), Albuquerque, NM (United States), Tech. Rep. SAND2006-2518, 2006.

[11] Y. Ojo, J. D. Watson, K. Laib, and I. Lestas, "A distributed scheme for voltage and frequency control and power sharing in inverter-based microgrids," *IEEE Transactions on Control Systems Technology*, 2023.


979-8-3315-8138-1